Subdivision using angle bisectors is dense in the space of triangles

Steve Butler Ron Graham

Abstract

Starting with any nondegenerate triangle, we can use an interior point of the triangle to subdivide it into six smaller triangles. We can repeat this process with each new triangle, and continue doing so over and over. We show that starting with any arbitrary triangle, the resulting set of triangles formed by this process contains triangles arbitrarily close (up to similarity) to any given triangle when the point that we use to subdivide is the incenter.

1 Introduction

Given a triangle and an interior point of the triangle, we can divide the triangle up into six smaller triangles, also called daughters, by drawing line segments (or Cevians) from the vertex through the interior point to the opposite side (see Figure 1). The process can then be repeated with each new triangle with its own corresponding interior point and again repeated over and over. When the interior point is the centroid (i.e., the intersection point of the lines joining the vertices of the triangles to the midpoints of the opposite sides) this process corresponds to barycentric subdivision.

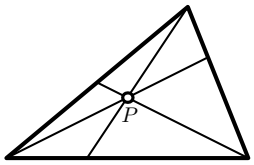

Figure 1: How to subdivide the triangle given an interior point P.

Stakhovskii asked whether repeated barycentric subdivision for a starting triangle is dense in the space of all triangles, i.e., the space of triangles up to similarity where two triangles are ε-close if the maximum difference between their corresponding angles is less than ε.[1] This question was answered in the affirmative.

Theorem 1 (Bárány-Beardon-Carne [3])**.** *Successive subdivisions of a non-degenerate triangle using the centroid point contains triangles which approximate arbitrarily closely (up to similarity) any given triangle.*

Moreover, it was shown that almost all triangles became "flat" in the sense that for $\varepsilon > 0$ at most ε portion of the triangles have the largest angle less than $\pi - \varepsilon$ after some finite number of successive subdivisions. Ordin [13] extended their results and showed that this also holds if we choose the interior point of the triangle to be $p_0A + p_1B + p_2C$ where A, B, C are the vertices

[1] When working in the space of similar triangles, the angles are unordered. For our purposes we will find it useful to work with triangles which have an order associated with the angles in the triangle so that triangles can be represented as vectors. However one should keep in mind that at the end we can then "mod" out by the natural symmetry of unordering the angles.

with $p_0 + p_1 + p_2 = 1$ and $p_i > 0$. This result assumes a labeling, i.e., an orientation, of the vertices which is consistent with the subdivision. When the point is the centroid, corresponding to $p_0 = p_1 = p_2 = \frac{1}{3}$, there is no ambiguity.

Our main result is to show that a similar statement holds if we choose the interior point to be the incenter. The incenter point corresponds to the center of the inscribed circle; it is also well known this point can be found by taking the intersection of the angle bisectors (an example of this is shown in Figure 9).

Theorem 2. *Successive subdivisions of a non-degenerate triangle continually using the incenter point contain triangles which approximate arbitrarily closely (up to similarity) any given triangle.*

The statements of the two theorems indicate that the different choices for subdivisions share a property in common. However, we will also show that there are differences. In particular, for the incenter we will show that most triangles do not become flat as happens when using the centroid.

We will proceed as follows. In Section 2 we will give a quick sketch of Theorem 1, while in Section 3 we will give a proof of Theorem 2 and establish several properties about this subdivision. Finally, in Section 4 we will give some remarks about other possible ways to subdivide triangles.

2 Subdividing using the centroid

In this section we give a quick sketch of the ideas behind Theorem 1. The method of Bárány et al. [3] was to first associate triangles with points in the hyperbolic half plane, $\mathbb{H}^2$. This is a model of geometry in the portion of the complex plane with positive imaginary part wherein straight lines correspond to circular arcs (including straight lines) which intersect the real axis perpendicularly. More information about hyperbolic geometry can be found in several places such as [2].

Given a triangle T, we associate the triangle with (up to) six points z in $\mathbb{H}^2$ as shown in Figure 2. This is done by placing *some* edge of T with vertices at $z = 0$ and $z = 1$ and the third vertex is located at the complex coordinate z with positive imaginary part.

The reason for using the hyperbolic half plane is that the relationship between the six different possible placements reduces to reflections. Namely, reflections across the three "lines" $\Re(z) = \frac{1}{2}$, $|z| = 1$, and $|z - 1| = 1$.

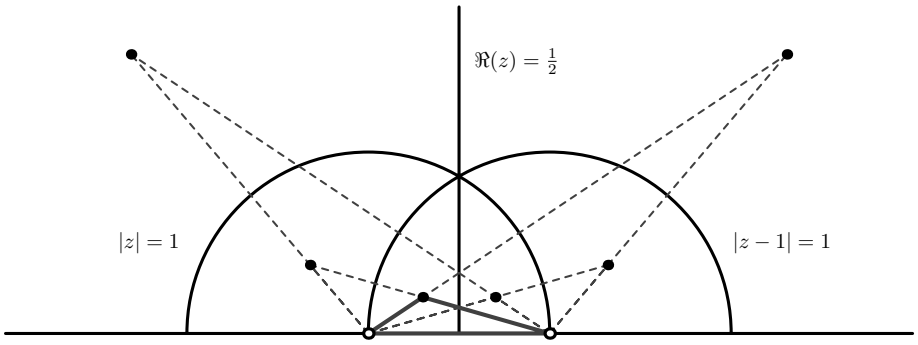

Figure 2: Triangles as points in the hyperbolic plane.

The centroid point of a triangle with vertices at 0, 1 and z is the point $(z+1)/3$, and so one of the corresponding daughters becomes $2(z+1)/3$ when the daughter is placed in $\mathbb{H}^2$. The argument for Theorem 1 now reduces to showing that the collection of automorphisms of $\mathbb{H}^2$ generated by combining the map $2(z+1)/3$ and the above reflections is dense in the set of all automorphisms of

$\mathbb{H}^2$. It follows for any starting z (i.e., any initial triangle T), the set of all resulting points which can be constructed by applying these maps (i.e., the daughters) is dense in $\mathbb{H}^2$ (i.e., dense in the space of triangles).

Further, using results of Furstenberg [8], it follows that almost all random walks formed from the operations of $2(z+1)/3$ and the reflections tend to infinity (in the hyperbolic half plane) as the length of the product increases. This then implies that almost all of the nth generation daughters have smallest angle tending to 0 as n increases. By different techniques, Hough [9] was able to show that the largest angle approaches π and moreover was able to give asymptotic bounds for the proportion of triangles with angles near π.

3 Subdividing using the incenter

The important step in the proof of Theorem 1 was to find a way to represent triangles as points in an auxiliary space having a natural action which corresponded to finding the daughters. The first step in proving Theorem 2 is to do the same. However, we will find it more convenient to associate each triangle with a point in $\mathbb{R}^3$ where the coordinates are the angles. The set of all possible triangles (including degenerate cases), denoted $\mathbf{P}$, is the intersection of the hyperplane $x + y + z = \pi$ with the first octant (see Figure 3). In this setting, we implicitly assume some ordering on the angles. As a result each triangle will correspond to up to six points in $\mathbf{P}$ when we drop the ordering.

We note that $\mathbf{P}$ is itself an equilateral triangle (see [1, 6, 11, 12] for previous applications involving $\mathbf{P}$).

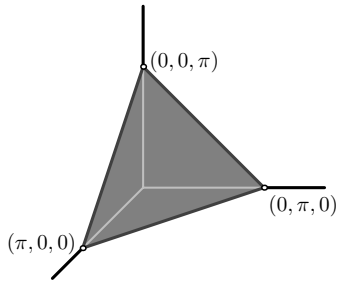

Figure 3: Representing triangles as points on $\mathbf{P}$ in $\mathbb{R}^3$.

As noted in the introduction, the incenter is found by the intersection of the angle bisectors. So the angles of the new triangles created by subdivision are linear combinations of the angles of the original triangles (hence the reason it is more convenient to work with $\mathbf{P}$). In particular, if we let the column vector $\mathbf{t} = [\alpha, \beta, \gamma]^T$ correspond to the triangle (α, β, γ), then the six new triangles are found by $M_i\mathbf{t}$ where

$$M_1 = \begin{pmatrix} 1/2 & 0 & 0 \\ 1/2 & 1/2 & 0 \\ 0 & 1/2 & 1 \end{pmatrix}, \quad M_2 = \begin{pmatrix} 1/2 & 1/2 & 0 \\ 0 & 1/2 & 0 \\ 1/2 & 0 & 1 \end{pmatrix}, \quad M_3 = \begin{pmatrix} 1 & 0 & 1/2 \\ 0 & 1/2 & 0 \\ 0 & 1/2 & 1/2 \end{pmatrix},$$
$$M_4 = \begin{pmatrix} 1 & 1/2 & 0 \\ 0 & 1/2 & 1/2 \\ 0 & 0 & 1/2 \end{pmatrix}, \quad M_5 = \begin{pmatrix} 1/2 & 0 & 1/2 \\ 1/2 & 1 & 0 \\ 0 & 0 & 1/2 \end{pmatrix}, \quad M_6 = \begin{pmatrix} 1/2 & 0 & 0 \\ 0 & 1 & 1/2 \\ 1/2 & 0 & 1/2 \end{pmatrix}.$$

Observation 1. *The union of the $M_i\mathbf{P}$ covers $\mathbf{P}$.*

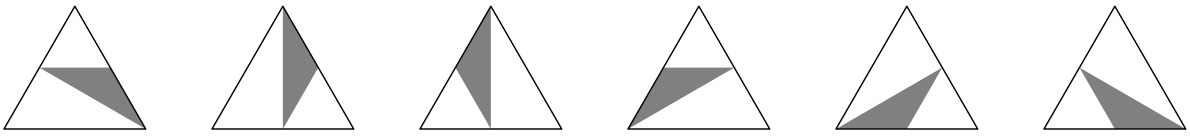

Figure 4: The image of $\mathbf{P}$ as a shaded region inside of $\mathbf{P}$ under the six maps M_i.

This can be seen by examining Figure 4. Alternatively, this says that every point in $\mathbf{P}$ has a preimage in $\mathbf{P}$ under some M_i. For the case that $\mathbf{t} = [\alpha, \beta, \gamma]^T$ with $\alpha \leq \beta \leq \gamma$, we have that $(M_1)^{-1}\mathbf{t} = [2\alpha, 2\beta - 2\alpha, \alpha - \beta + \gamma]^T$ is a preimage of $\mathbf{t}$ in $\mathbf{P}$. For each other possible ordering of the angles, there is an M_i which will similarly show the existence of a preimage.

Observation 2. *If we let $\|\cdot\|$ denote Euclidean distance, then $\|M_i(\mathbf{t} - \mathbf{s})\| \leq \frac{\sqrt{3}}{2}\|\mathbf{t} - \mathbf{s}\|$.*

To see this we can put $\mathbf{P}$ into $\mathbb{R}^2$ by $\mathbf{t} = [\alpha, \beta, \gamma]^T \to \left[\frac{\alpha+2\beta}{\sqrt{3}}, \alpha\right]^T$; note that this will preserve distance. Under this map we would also have that $M_1\mathbf{t} \to \left[\frac{3\alpha+2\beta}{2\sqrt{3}}, \frac{\alpha}{2}\right]^T$. If we now let $\mathbf{s} = [\alpha', \beta', \gamma']^T$, then a calculation shows

$$\frac{3}{4}\|\mathbf{t} - \mathbf{s}\|^2 - \|M_1(\mathbf{t} - \mathbf{s})\|^2 = \frac{2}{3}\big(\beta - \beta'\big)^2 \geq 0.$$

The result now follows for M_1 and similar calculations establish it for the remaining M_i.

We now prove Theorem 2 which will immediately follow from the two above observations about the properties of the maps M_i. Let $\mathbf{q}$ be the initial triangle we apply subdivision to. We need to show that for any triangle $\mathbf{t}$ and $\varepsilon > 0$ there is some sequence of i_j so that

$$\big\|(M_{i_1}M_{i_2}\cdots M_{i_k}\mathbf{q}) - \mathbf{t}\big\| < \varepsilon.$$

Choose k sufficiently large so that $\pi\sqrt{2}\big(\frac{\sqrt{3}}{2}\big)^k < \varepsilon$. By Observation 1, we can successively find a kth generation preimage of $\mathbf{t}$ in $\mathbf{P}$, which corresponds to multiplying by an appropriate $(M_i)^{-1}$ at each step. Denote this preimage by

$$(M_{i_k})^{-1}\cdots(M_{i_2})^{-1}(M_{i_1})^{-1}\mathbf{t},$$

(where the i_j are chosen according to how we construct the preimage). Repeatedly using Observation 2 we have

$$\begin{aligned}
\big\|(M_{i_1}M_{i_2}\cdots M_{i_k}\mathbf{q}) - \mathbf{t}\big\| &= \big\|M_{i_1}\big(M_{i_2}\cdots M_{i_k}\mathbf{q} - (M_{i_1})^{-1}\mathbf{t}\big)\big\| \\
&\leq \frac{\sqrt{3}}{2}\big\|M_{i_2}\cdots M_{i_k}\mathbf{q} - (M_{i_1})^{-1}\mathbf{t}\big\| \\
&\leq \cdots \\
&\leq \big(\frac{\sqrt{3}}{2}\big)^k\big\|\mathbf{q} - (M_{i_k})^{-1}\cdots(M_{i_2})^{-1}(M_{i_1})^{-1}\mathbf{t}\big\| \\
&\leq \pi\sqrt{2}\big(\frac{\sqrt{3}}{2}\big)^k \;<\; \varepsilon.
\end{aligned}$$

In the last step we used that points in $\mathbf{P}$ are at most distance $\pi\sqrt{2}$ apart. This finishes the proof of Theorem 2.

The limiting distribution

In fact, more can be said about the iterated subdivision of triangles using the incenter. Namely, since the maps M_i are contracting at each stage at least by a factor of $\sqrt{3}/2$ then it follows (see [7]) that there is a fixed limiting distribution on $\mathbf{P}$ that the process converges to. Further it converges exponentially.

To get some sense of what this limiting distribution looks like, we can simply start with any triangle (in our case we will use an equilateral triangle) and plot all of the nth generation daughters for some n in $\mathbf{P}$. This is done for $n = 5$ in Figure 5a.

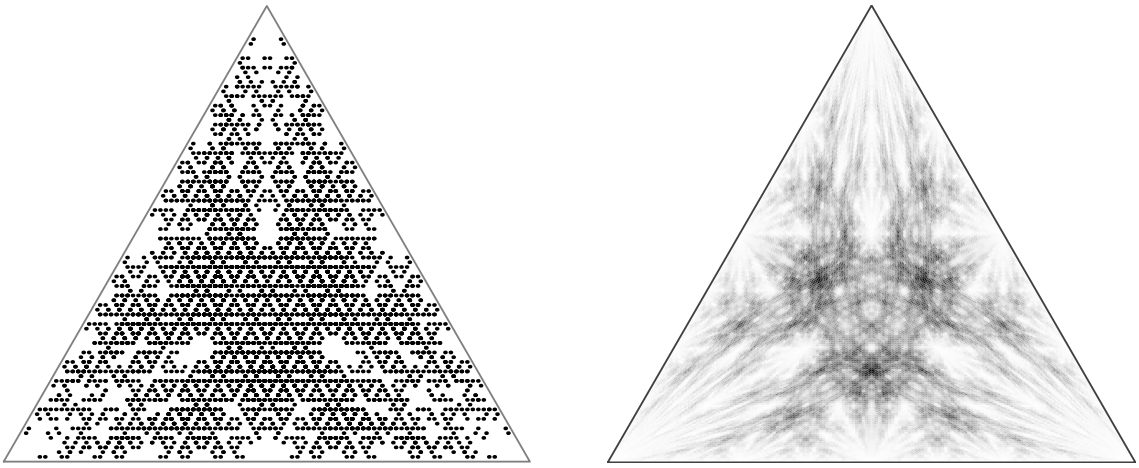

(a) (b)

Figure 5: The distribution of the nth generation daughters using the incenter.

Examining Figure 5a, we see that the daughters seem to fill in most of $\mathbf{P}$ (agreeing with Theorem 2). However, a patient count will reveal that there are far fewer than 6^5 points (i.e., triangles) in Figure 5a. This is because some points have been mapped onto several times (a consequence of starting with such a symmetric triangle). So to get a better sense of the limiting distribution, instead of plotting the individual points in $\mathbf{P}$ it is better to look at a histogram. We will divide $\mathbf{P}$ into a large number of small regions and then shade each region according to the number of points that fall into that region, the darker a region is the more points fall into that region. In Figure 5b we give the histogram for $n = 12$ generations starting with the equilateral triangle.

Very little is known about the limiting distribution. Experimentally, it appears that the densest point on the limiting distribution (i.e., the darkest region in Figure 5b) corresponds to $[\frac{\pi}{5}, \frac{\pi}{5}, \frac{2\pi}{5}]^T$. This is likely because this is an eigenvector of eigenvalue 1 of two of the M_i. In other words, under subdivision using the incenter the corresponding triangle has two of its daughters which are similar to it (see Figure 6). No other triangle has this property, and the triangle corresponding to the vector $[\frac{2\pi}{9}, \frac{3\pi}{9}, \frac{4\pi}{9}]^T$ is the only other triangle with one of its daughters similar to itself, but this triangle does not appear to play as significant a role in the distribution.

If we were to draw the histogram for $n = 20$ or $n = 50$ and compare it to Figure 5b, we would see almost no perceptible difference between them. This is because, as we noted above, the convergence to the limiting distribution is exponential. Or put another way, if we look at what happens when we map a triangle under n applications of the M_i in $\mathbf{P}$, then knowing the last few steps that we applied gives us a good handle on where we are in $\mathbf{P}$. This is essentially the heart of the proof of

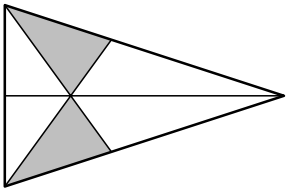

Figure 6: The triangle $[\frac{\pi}{5}, \frac{\pi}{5}, \frac{2\pi}{5}]^T$ subdivided using the incenter (the shaded triangles are similar to the original).

Theorem 2.

For example, if we consider what happens when $\mathbf{P} \to M_1M_2M_3\mathbf{P}$, we see that $\mathbf{P}$ will map to a region with vertices $[\frac{\pi}{4}, \frac{\pi}{4}, \frac{\pi}{2}]^T$, $[\frac{\pi}{8}, \frac{\pi}{4}, \frac{5\pi}{8}]^T$ and $[\frac{\pi}{8}, \frac{\pi}{8}, \frac{3\pi}{4}]^T$. It follows that for any triangle $\mathbf{t}$ that $M_1M_2M_3(\cdots)\mathbf{t}$ must lie in this subregion of $\mathbf{P}$, i.e., $1/6^3$ of the descendant daughters of $\mathbf{t}$ will be in this subregion. Since points inside this subregion of $\mathbf{P}$ have minimum angle at least $\pi/8$, we have shown at least $1/6^3$ of the daughters in the nth generation must have minimum angle at least $\pi/8$.

In Figure 7a, 7b and 7c we have plotted all of the regions $\mathbf{P}$ maps to under all possible second ($M_iM_j\mathbf{P}$), third ($M_iM_jM_k\mathbf{P}$) and fourth ($M_iM_jM_kM_\ell\mathbf{P}$) generation maps. (The number of such regions is large so it is difficult to pick out the individual regions; nevertheless there is a strong similarity with the histogram in Figure 5b.)

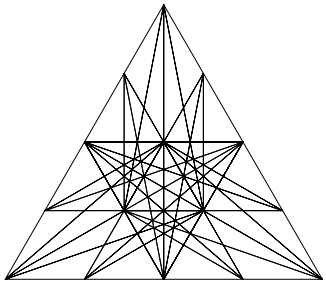

(a) Second generation

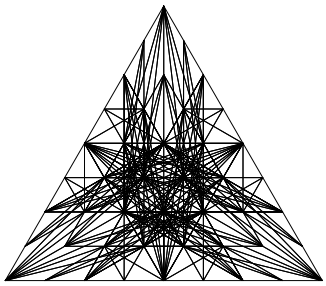

(b) Third generation

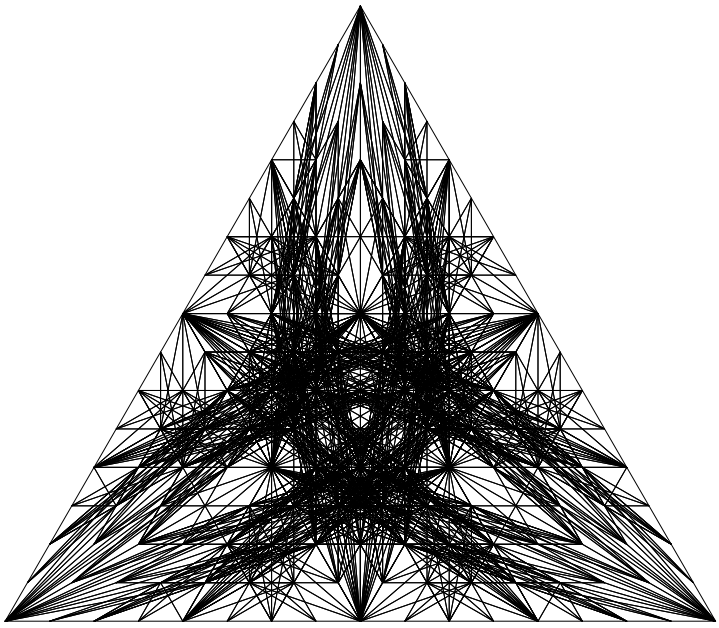

(c) Fourth generation.

Figure 7: Resulting images of $\mathbf{P}$ for different generations.

Of course, by looking at larger products and looking over more prefixes we gain more information about what happens with the minimum angle. We can get numerical bounds for the limiting cumulative distribution function, or CDF, for the smallest angle in a triangle. That is, we can estimate the limiting proportions of triangles that have minimum angle $\leq \theta$ for $0 \leq \theta \leq \frac{\pi}{3}$. This is done by considering all resulting 6^n regions which correspond to images of $\mathbf{P}$ in the nth generation.

Given a θ, for the lower bound of the CDF we count the proportion of images in $\mathbf{P}$ which have

the largest minimum angle at most θ. For the upper bound we count the proportion of images in $\mathbf{P}$ which contain a minimum angle at most θ. When this is done using the regions for $n = 11$, the resulting upper and lower bounds for the CDF are as given in Figure 8. (By comparison the limiting CDF under subdivision using centroids is the constant function 1, showing that these two methods of subdividing are fundamentally different.)

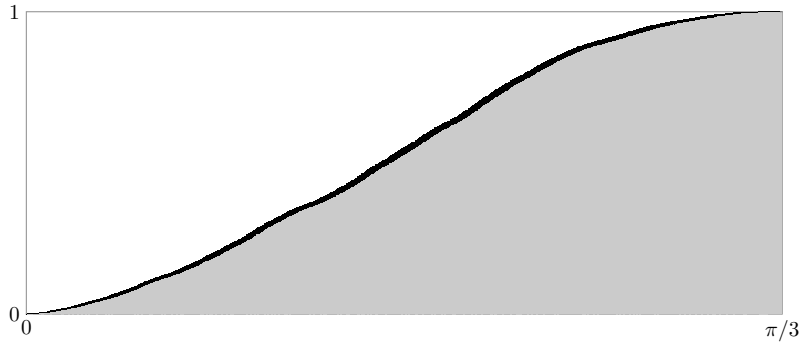

Figure 8: Upper and lower bounds for the CDF for the smallest angle in the limiting distribution.

4 Comparison with other methods of subdivision

We have seen that like the centroid, when doing subdivision using the incenter the resulting triangles are dense in the space of all triangles. However, unlike the centroid, the smallest angle in a typical triangle does not tend to 0. This is important since certain applications can fail when the subdivision creates a large number of triangles with minimal angles going to 0 as n gets large (see [4, 14, 15]).

One interesting question is to understand properties of the limiting distribution of points in $\mathbf{P}$ for repeated subdivision when using the incenter, a good approximation of which was shown in Figure 5b.

One can also consider what happens for subdivision using other interior points. For example, the Gergonne point is found by taking the inscribed circle in the triangle and connecting a vertex to the point of tangency on the opposite edge; these three lines intersect at the Gergonne point (see Figure 9a; the triangle used has sides proportional to 19, 40 and 49 and is the unique triangle where one of the resulting daughters is an equilateral triangle).

When using the Gergonne point to subdivide, it is known [5] that the triangles are not dense in the space of all triangles. In Figure 10a we have given a histogram of $\mathbf{P}$ for the tenth generation of subdividing using the Gergonne point (including large white regions where there are no points).

An interesting point for which little is known about what happens after repeated subdivision is the Lemoine point, which corresponds to the intersection of the symmedians. The symmedians (solid lines in Figure 9b) are found by taking the medians (dashed lines in Figure 9b) and flipping them across the angle bisectors (dotted lines in Figure 9b). For comparison the centroid, incenter and Lemoine point have all been marked in Figure 9b.

In Figure 10b we have given a histogram of $\mathbf{P}$ for the eleventh generation of subdividing using the Lemoine point. It is currently unknown if this method of subdivision is dense in the space of all triangles and what the limiting behavior is (there is some experimental evidence that the triangles become flat, but the convergence seems to be relatively slow).

More information about the Gergonne and Lemoine points, as well as a large number of other interesting points available to investigate, can be found online (see [10]). More information about what happens under repeated subdivision using a central point can be found in [6].

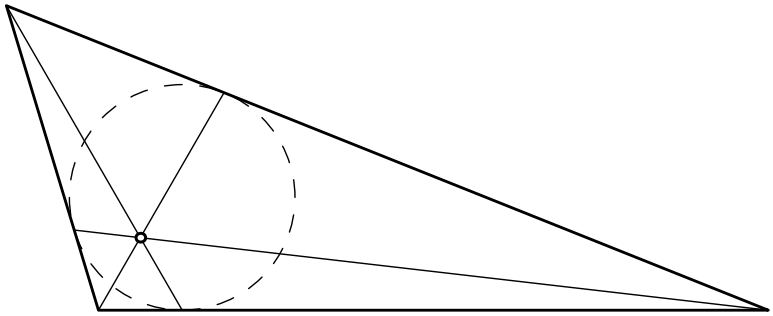

(a) Gergonne point

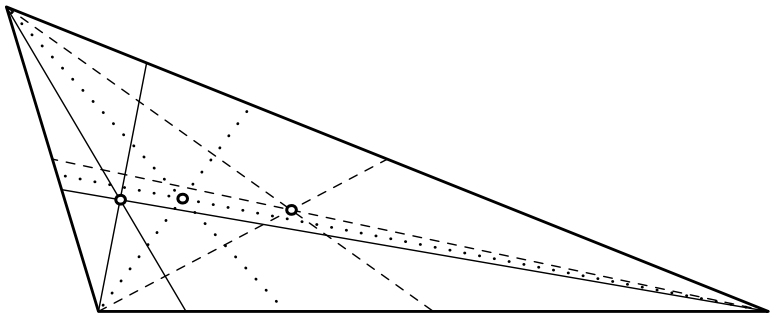

(b) Centroid (dashed lines), incenter (dotted lines), and Lemoine (solid lines) points

Figure 9: Constructions for the Gergonne and Lemoine points.

References

[1] J. C. Alexander, The symbolic dynamics of pedal triangles, *Math. Mag.* **66** (1993) 147–158.

[2] J. W. Anderson, *Hyperbolic Geometry*, Springer, New York, 1999.

[3] I. Bárány, A. F. Beardon, T. K. Carne, Barycentric subdivision of triangles and semigroups of Möbius maps, *Mathematika* **43** (1996) 165–171.

[4] M. Bern, D. Eppstein, Mesh generation and optimal triangulation, in *Computing in Euclidean Geometry*, Edited by D.-Z. Du and F. Hwang, World Scientific Publishing, River Edge, NJ, 1992. 23–90.

[5] S. Butler, The lost daughters of Gergonne, Forum Geometricorum **9** (2009) 19–26.

[6] S. Butler, R. Graham, Iterated triangle partitions, in *Fete of Combinatorics and Computer Science*, Edited by G. Katona, A. Schrijver and T. Szonyi, Bolyai Society Mathematical Studies 29, Springer-Verlag, Heidelberg, 2010. 23–42.

[7] P. Diaconis, D. Freedman, Iterated random functions, *SIAM Review* **41** (1999) 45–76.

[8] H. Furstenberg, Noncommuting random products, *Trans. Amer. Math. Soc.* **108** (1963) 377–428.

[9] R. Hough, Tesselation of a triangle by repeated barycentric subdivision, *Elect. Comm. in Probab.* **14** (2009) 270–277.

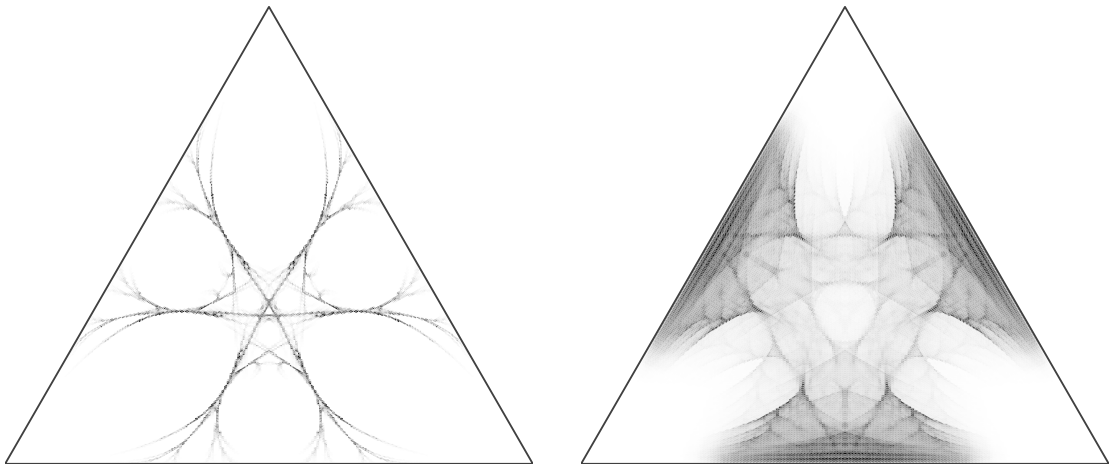

(a) Gergonne point (b) Lemoine point

Figure 10: Histograms for the Gergonne and Lemoine points.

[10] C. Kimberling, Encyclopedia of Triangle Centers (2012), available at `http://faculty.evansville.edu/ck6/encyclopedia/ETC.html`

[11] J. Kingston, J. Synge, The sequence of pedal triangles, *Amer. Math. Monthly* **95** (1988) 609–620.

[12] P. Lax, The ergodic character of sequences of pedal triangles, *Amer. Math. Monthly* **97** (1990) 377–381.

[13] A. A. Ordin, A generalized barycentric subdivision of a triangle, and semigroups of Möbius transformations, *Russian Math. Surveys* **55** (2000) 591–592.

[14] M. Rivar, G. Iribarren, The 4-triangles longest-side partition of triangles and linear refinement algorithms, *Math. of Computation* **65** (1996) 1485–1502.

[15] I. Rosenberg, F. Stenger, A lower bound on the angles of triangles constructed by bisecting the longest side, *Math. of Computation* **29** (1975) 390–395.

STEVE BUTLER received his Ph.D. from the University of California, San Diego in 2008 under the direction of Fan Chung. After holding an NSF Mathematical Sciences Postdoctoral Fellowship at UCLA he came to Iowa State University where he is currently an Assistant Professor in the Department of Mathematics.
Department of Mathematics, Iowa State University, Ames, IA 50011, USA
butler@iastate.edu

RON GRAHAM is the Irwin and Joan Jacobs Professor in the Department of Computer Science and Engineering and the Chief Scientist of California Institute for Telecommunications and Information Technology. He is a former president of the Mathematical Association of America and the American Mathematical Society and has been awarded numerous honors for his extensive groundbreaking work in discrete mathematics. Most recently he co-wrote *Magical Mathematics* with Persi Diaconis which was awarded the 2013 Euler Book Prize.

Department of Computer Science and Engineering, University of California, San Diego, La Jolla, CA 92093, USA
graham@ucsd.edu